Amphiphilicity Determines Binding Properties of Three Mitochondrial Presequences to Lipid Surfaces†

P. K. Hammen,‡,|| D. G. Gorenstein,§ and H. Weiner*,‡

Department of Biochemistry, Purdue University, West Lafayette, Indiana 479070-1153, and Department of Human Biological Chemistry and Genetics, University of Texas, Medical Branch, Galveston, Texas 77555

Received August 9, 1995; Revised Manuscript Received January 24, 1996⊗

ABSTRACT: The interactions of three peptides, which correspond to presequences that direct mitochondrial protein import, with model membrane systems were characterized using NMR, fluorescence, and circular dichroism spectroscopies. The positively charged peptides adopted an ordered secondary structure only when the negatively charged phospholipid, cardiolipin, was present in small unilamellar vesicles. Conversely, the peptides adopted an ordered secondary structure in the presence of micelles formed from both formally neutral and negatively charged detergents. The peptides had the same relative affinity for micelles and small unilamellar vesicles containing 20% cardiolipin. Amide proton exchange rates showed that the region of the helical structure which had the greatest hydrophobic moment interacted most readily with micelles. Therefore, it appears that a major determinant of binding to lipid surfaces is the ability of the peptide to attain the correct orientation of hydrophobic and hydrophilic groups. For the three peptides studied, affinity also correlated with the length of the helix, but not with hydrophobic surface area. In each case, the interacting segment of the peptide was toward the C-terminal end of the helix. Previous work has allowed us to postulate that the N-terminus of the presequence is vital for import [Wang, Y., & Weiner, H. (1993) *J. Biol. Chem. 268*, 4759−4765] and the C-terminal end is essential for membrane interaction [Karslake, C., Piotto, M., Pak, Y. K., Weiner, H., & Gorenstein, D. G. (1990) *Biochemistry 29*, 9872−9878]. On the basis of the data that are now available, it appears that the interaction with membrane surfaces may depend on the location of an amphiphilic region of the sequence that is near but not necessarily at the C-terminus.

Polypeptides interact with membranes in numerous biological processes. These include the translocation of proteins across membranes (Wickner, 1988), the insertion of membrane proteins into the membrane (Saier *et al*., 1989; Cramer *et al*., 1992), and the action of peptide hormones at the membrane surface (Schwyzer, 1991). Significant effort has been devoted to studying the peptide−membrane interaction (Roise, 1993), yet it is not completely understood. One type of protein that is capable of interacting with membranes is the family of nuclear-encoded proteins that are synthesized in the cytosol and subsequently translocated across one or both mitochondrial membranes. These proteins possess N-terminal presequences which are required for protein translocation. Upon comparison, they display no primary sequence homology but generally have a net positive charge. It has been proposed that the presequences must be able to form amphiphilic secondary structures, with charged and hydrophilic side chains distributed about one surface of the polypeptide and nonpolar side chains about the opposite surface (von Heijne, 1986; Roise *et al*., 1988). Due to the organization of phospholipids in the membrane, the amphiphilic polypeptides are well-suited for interaction at a membrane surface.

Presequences must be capable of interacting specifically with mitochondrial protein components other than just the membranes. Results from competition experiments with presequence peptides suggest that they interact with import receptor proteins located in the outer membrane (Glaser & Cumsky, 1990; Pak *et al*., 1990; Vallette *et al*., 1994). Binding experiments show that the interaction of some precursor proteins with yeast mitochondria is eliminated upon deletion of the receptor gene and that this interaction is dependent on salt concentration (Haucke *et al*., 1995). The presequence also interacts with the processing protease that removes it after import (Ou *et al*., 1989). Secondary structure is believed to be important for these interactions, as well (Wang & Weiner, 1993; Hammen *et al*., 1994). It is not known, though, if the presequence interacts with cytosolic proteins or the various heat shock proteins involved in some aspects of import and processing. However, the binding of a N-terminal synthetic peptide from a mitochondrial protein to the *Escherichia coli* chaperonin, GroEL, has been demonstrated (Landry & Gierasch, 1991). The peptide adopted an α-helical conformation when bound to GroEL. Knowledge of the different environments that will induce

† This work was supported in part by NIH Grant AA05812 (H.W.) and by NIH Grant AI27744 (D.G.G.). P.K.H. was supported by NIH Training Grant 5T32DK07532. H.W. was a recipient of Senior Scientist Award AA00028 from the National Institutes on Alcohol Abuse and Alcoholism. This is journal paper number 14928 from the Purdue Agricultural Experiment Station.

* Corresponding author: Dr. Henry Weiner, Department of Biochemistry Purdue University West Lafayette, Indiana 47907-1153.

‡ Purdue University.

§ University of Texas, Medical Branch.

|| Author to whom inquiries should be addressed.

⊗ Abstract published in *Advance ACS Abstracts,* March 15, 1996.

0006-2960/96/0435-3772$12.00/0

secondary structure formation in mitochondrial presequences will be useful for understanding how the presequences function.

Biological membranes typically contain a complex mixture of phospholipids, cholesterol, proteins, and various other substances. Because of this diversity, it is difficult to study peptide binding to intact biological membranes and obtain results that can be attributed to a specific interaction. Artificial membrane materials such as monolayer films or phospholipid vesicles provide a more clearly defined experimental system (De Kroon *et al*., 1993). With these artificial membrane systems, information has been obtained on binding thermodynamics (Myers *et al*., 1987; Kim *et al*., 1991) and on the orientation of the peptide when bound (Snel *et al*., 1995). Due to their large mass and irregular nature, these model systems are generally not conducive to high-resolution structural techniques such as NMR spectroscopy or X-ray crystallography. For this reason, detergent micelles have been used as a membrane-mimetic material in NMR studies (Braun *et al*., 1981; Gierasch *et al*., 1982). Micelles provide a lipid-like site for interaction of peptides while maintaining a size that is amenable to high-resolution NMR methods. The limitations of micelles are that they do not form a lipid bilayer, that they have a more highly curved surface than the typical membrane due to their small size, and that lipid molecules do not pack together as tightly as they do in a bilayer (Dill & Flory, 1981). Although reasonable peptide NMR spectra are often obtained from studies with micelles, it is not always clear to what extent micelles accurately represent more realistic membrane models. For example, peptides have been shown to form distorted α-helices upon interaction with micelles (Braun *et al*., 1981; Thornton & Gorenstein, 1994). It is not certain whether these distortions are a conformational characteristic of the peptide or a consequence of the interaction with micelles that is somehow different from the interaction that would occur with a lipid bilayer at a flatter membrane surface.

In this study, we have utilized NMR, circular dichroism, and fluorescence spectroscopies to investigate mitochondrial presequence characteristics in the presence of structure-inducing model membrane systems. Three different peptides were used which, when located at the N-terminus, share the function of targeting precursor proteins to mitochondria for import. Each has been shown to form a continuous α-helical structure containing at least three turns when in contact with DPC[1] micelles (Thornton *et al*., 1993; Hammen *et al*., 1994). Two of the peptides correspond to the N-terminal segments from rat mitochondrial rhodanese and from 3-oxoacyl-CoA thiolase, and the third represents a deletion mutant of the presequence of rat liver mitochondrial aldehyde dehydrogenase [ALDH(−RGP)]. The amino acid sequences are shown in Figure 1. While the sequences all function in import, there are significant differences among them. The lengths of the helical segments of thiolase[1−21], ALDH(−RGP), and rhodanese[1−23] are approximately three, four, and five turns, respectively. Another difference can be seen in helical wheel diagrams which are also shown in Figure 1. They indicate that, in the experimentally observed α-helical regions, the three peptides display very different distributions of hydrophobic and hydrophilic side chains about the helical axis. These patterns suggest different amphiphilic characteristics which should lead to a corresponding difference in their abilities to interact with membrane-mimetic materials. We have compared and evaluated the interaction of these peptides with micelles and SUVs to ascertain common features and present experimental evidence that the amphiphilicity of the peptides is the major factor that determines the affinity of interaction with these model membrane systems.

[1] Abbreviations: ALDH, aldehyde dehydrogenase; DPC, dodecylphosphocholine; DPC-d_{38}, perdeuterated dodecylphosphocholine; SUV, small unilamellar vesicle; SDS, sodium dodecyl sulfate; CL, cardiolipin; TOCSY, total coherence spectroscopy; NOESY, nuclear Overhauser effect spectroscopy.

MATERIALS AND METHODS

Chemicals. CL and SDS were purchased from Sigma. L-α-Lecithin was from Avanti Polar Lipids. DPC-d_{38} was purchased from MSD Isotopes. Deuterium oxide (99.9% minimum isotope enrichment) was purchased from Cambridge Isotope Laboratories.

Peptide Synthesis and Purification. Peptides were synthesized in the Purdue University Biochemistry Department Laboratory for Macromolecular Structure using an ABI 430A solid state peptide synthesizer. The peptides were purified using a semipreparative Vydac C_{18} reverse phase (20 cm × 1 cm diameter) high-performance liquid chromatography column. Peptide elution was achieved by the application of a linear acetonitrile gradient of 5 to 60% at a rate of approximately 2%/min. Peptide authenticity was determined by mass spectrometry in the Purdue University Campus-Wide Mass Spectrometry Center and verified by amino acid analysis in the laboratory of Prof. Michael Laskowski of the Purdue University Department of Chemistry. Peptide concentrations in aqueous buffer were calculated from the amino acid concentrations determined by the amino acid analysis.

Circular Dichroism. Circular dichroism (CD) spectra were obtained on a Jasco J-600 spectropolarimeter, which was typically scanned from 250 to 190 nm at 25 °C. The path length for the samples was 0.1 cm. Baseline spectra for each solvent were obtained prior to the peptide spectra. Peptide concentrations in these measurements were 10, 28, and 30 μM for rhodanese[1−23], thiolase[1−21], and ALDH(−RGP), respectively. The concentration of lipid in the micellar solutions was 20 mM, which was above the critical micelle concentration and was sufficient to ensure an excess of micelles to peptide molecules. For solutions of SUVs, the lipid concentration could not exceed 0.25 mM because of the noise in the CD spectrum caused by the vesicles. The secondary structure analyses were carried out using a nonlinear least squares fit of the experimental spectra to standard values derived from a data base of protein CD spectra (Yang *et al*., 1986).

Nuclear Magnetic Resonance. All nuclear magnetic resonance spectra were obtained on a Varian VXR-500 spectrometer. Peptide samples were approximately 2 mM, DPC-d_{38} was 200 mM, and the solution was buffered with 50 mM phosphate (pH 3.3). The high concentration of detergent was to assure that an excess of micelles would be present in the solution (Opella *et al*., 1994). No sign of multiple conformers was apparent in any of the spectra.

A

rhodanese[1-23] M-V-H-Q-V-L-Y-R-A-L-V-S-T-K-W-L-A-E-S-I-R-S-G

thiolase[1-21] M-A-L-L-R-G-V-F-I-V-A-A-K-R-T-P-F-G-A-Y-G

ALDH(-RGP) M-L-R-A-A-L-S-T-A-R-R-L-S-R-L-L-S-Y-A

B

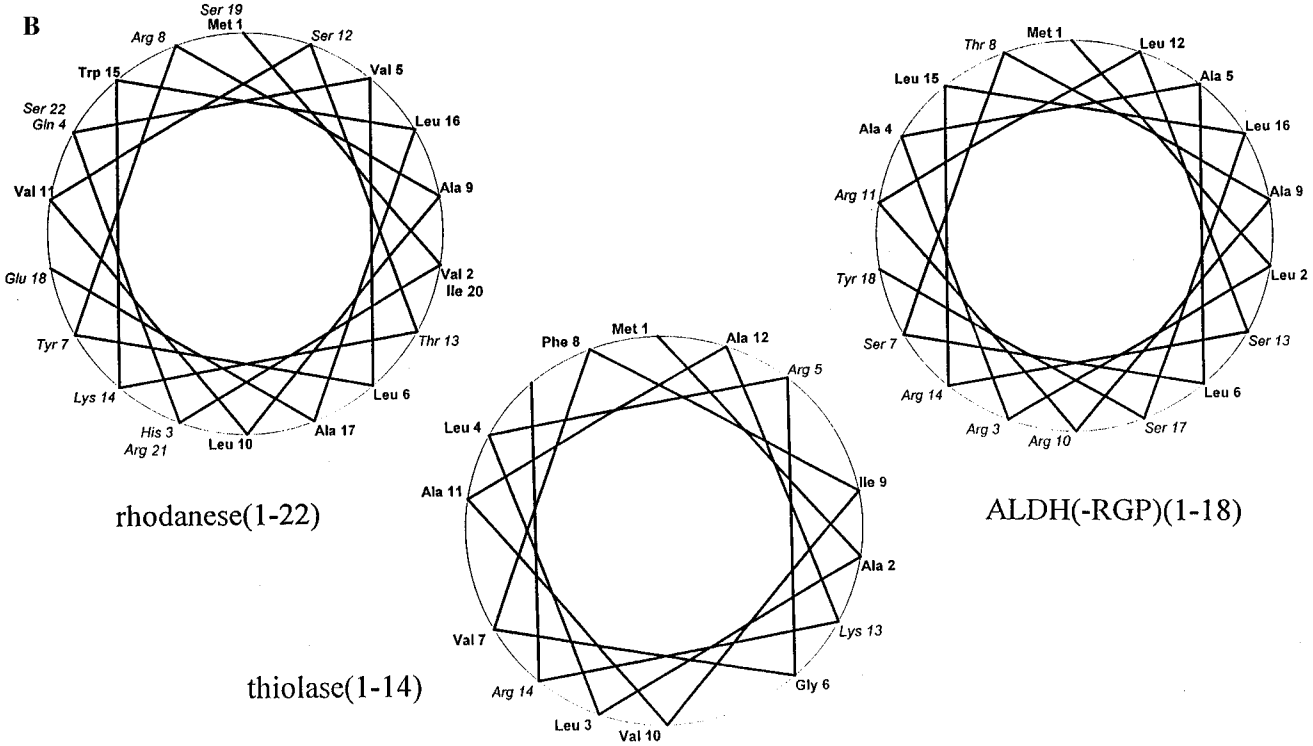

FIGURE 1: (A) Amino acid sequences of the presequence peptides used. Underlined portions of the sequences have been determined to be helical in the presence of micelles (Thornton *et al.*, 1993; Hammen *et al.*, 1994). (B) Helical wheel diagrams representing the helical portion of each sequence. Three-letter abbreviations for the amino acids along with the sequence number are used at each position of the helical wheel. Hydrophobic residues appear in bold print.

Spectral assignments were made for rhodanese[1−23] in the presence of micelles, using data in DQF-COSY (Piatini *et al.*, 1982), TOCSY (Braunschweiler & Ernst, 1983; Bax & Davis, 1985), and NOESY (Jeener *et al.*, 1979) spectra. The two-dimensional spectra were obtained with a spectral width of 6000 Hz in both f_1 and f_2 in 2K complex data sets. A total of 300 t_1 increments, 32 scans each, were obtained using the hypercomplex method to achieve quadrature detection in the f_1 dimension (States *et al.*, 1982). TOCSY data were obtained using a 32 ms MLEV-16 mixing sequence to achieve coherence transfer. NOESY data were obtained with a 150 ms mixing time. Fourier transformation was weighted with a sine-bell function shifted 60°. All chemical shifts were referenced to an internal standard of perdeuterio sodium 3-(trimethylsilyl)-1-propane sulfonate (DSS). The temperature for all NMR spectra was 20 °C. Data sets were processed on SUN 4 workstations using VNMR software provided by Varian Associates, Inc.

Measurements of amide proton exchange were made by two different procedures which will be referred to as method I and method II. The principal difference between the two methods was in the state of the peptide when it was dissolved in ^2H_2O. For method I, the protonated peptide was dissolved in aqueous phosphate buffer (0.050 M, pH 4.2) which contained DPC-d_{38}. The solution was lyophilized and redissolved in 0.7 mL of ^2H_2O which gave an uncorrected pH of 3.5. The solid material typically dissolved in 2−4 min, after which it was transferred to a NMR tube. For method II, protonated peptide was dissolved in 0.35 mL of ^2H_2O. This solution was immediately added to a 0.35 mL solution which contained 0.4 M DPC-d_{38} dissolved in ^2H_2O. After a short period of gentle mixing, the solution was transferred to a NMR tube. This procedure typically took 2−4 min.

Using these methods, two different initial states were generated. The first state was the preformed peptide−micelle complex (method I). The second involved uncomplexed micelle and peptide, initially, and monitored exchange in competition with the formation of the complex (method II). Measuring NH exchange of the peptide−micelle complex under these two conditions allowed the distinction between the complex at equilibrium and in the presence of transiently formed states. Method I was used to observe characteristics of the intact peptide−micelle complex. Method II monitored the formation of the complex as well as exchange within the complex. If complex formation was very rapid compared to the rate of amide proton exchange, the same protons observed to be protected from solvent in method I would appear to be protected in method II (Scheme 1). However, if complex formation was rapid compared to amide proton exchange and there was an intermediate state with a lifetime on the order of amide proton exchange, a different pattern of amide proton protection could be observed in method II (Scheme 2).

Scheme 1

$$P + M \rightleftharpoons PM$$

Scheme 2

$$P + M \rightleftharpoons P{-}M \rightleftharpoons PM$$

For both methods I and II, after mixing, the sample was inserted into the magnetic field, the probe was tuned, and low-order axial shims were optimized. Acquisition parameters specific to the sample were optimized, and data collection was begun. Each two-dimensional data set, either TOCSY or NOESY, required 2 h for acquisition. Upon completion of one data set, the acquisition of the next was begun. The final experiment for thiolase[1−21] and ALDH(−RGP) was obtained after 12 h and for rhodanese[1−23] after 20 h from the time of mixing. After data processing, intensities were measured for individual NH−Hα cross-peaks. Rate constant estimates were obtained by plotting ln I_t versus time and fitting the points to the linear equation

$$\ln I_t = -k_{ex}t + \ln I_o$$

I_t is the measured intensity at time t which is the time at which each experiment was started.

For the exchange experiments, the two-dimensional spectra were obtained with a spectral width of 6000 Hz in both f_1 and f_2 in 2K complex data sets. A total of 256 t_1 increments, 8 scans each, were obtained using the hypercomplex method to achieve quadrature detection in the f_1 dimension. TOCSY data were obtained using a 30 ms MLEV-16 mixing sequence to achieve coherence transfer. NOESY data were obtained with a 100 ms mixing time. Fourier transformation was weighted with a sine-bell function shifted 60°. Where necessary, interference from the solvent resonance was reduced by identification and subtraction low-frequency components from the free induction decay before transformation (Smallcombe, 1993).

SUVs. SUVs were prepared as previously described (Hammen *et al*., 1994). The one exception was in the CL solution, which was 10 mg/mL in $CHCl_3$. The SUVs contained 20% CL, by weight.

Fluorescence Spectroscopy. Fluorescence spectra were obtained at 25 °C using a Hitachi F-2000 fluorescence spectrophotometer as previously described (Wang & Weiner, 1994). The tyrosine excitation wavelength was 272 nm. Tyrosine emission was monitored from 290 to 350 nm, with maxima between 304 and 308 nm. The excitation wavelength used for the tryptophan in rhodanese[1−23] was 288 nm. This wavelength was selected to excite Trp15 and minimize the excitation due to Tyr7 in the peptide. Tryptophan emission was monitored between 320 and 400 nm, with maxima between 335 and 355 nm, depending on the lipid concentration. The peptide concentrations were between 1 and 2 μM. For some titrations, the total solution volume increased by 5%. Therefore, corrections were made for dilution effects in all the titrations. When the peptide−lipid interaction had reached a state of saturation, 8−10 additional data points were obtained. The change in intensity with concentration, observed for these points, was linear. The slope of this line was used to make a correction for the effects of addition of lipid alone to the cuvette.

Molecular Modeling. Structures were generated and calculations were carried out using QUANTA 4.1 on a Silicon Graphics Indigo^2 workstation. For solvent accessible surface area calculations, a probe with a radius 1.4 Å was rolled over the surface of the molecular structure.

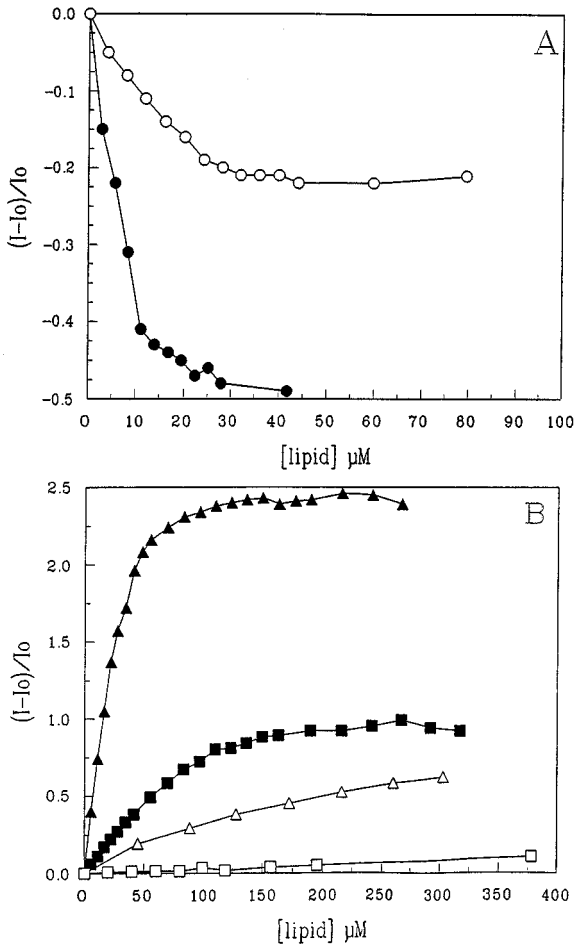

FIGURE 2: Fluorescence differences for (A) rhodanese[1−23] (○) and (B) thiolase[1−21] (□) and ALDH(−RGP) (△) when titrated with SUVs containing 100% egg L-α-lecithin (open symbols) or 20% CL/80% egg L-α-lecithin (closed symbols) at 25 °C. Peptides were dissolved in 2 mL of aqueous phosphate buffer (50 mM, pH 5.2) to a final concentration of 1−2 μM. Vesicle solutions were added in aliquots ranging from 1 to 5 μL until the fluorescence change neared zero. The data for egg L-α-lecithin SUVs with ALDH(−RGP) were taken from the Ph.D. Dissertation of Yi Wang (Wang, 1994).

RESULTS

Fluorescence Measurements. Differences in the fluorescence of either tyrosine or tryptophan side chains were used to measure the relative affinity of the three peptides for SUVs. Two different lipid compositions were used in the preparation of the SUVs, 0% CL/100% L-α-lecithin and 20% CL/80% L-α-lecithin. Percentages are on the basis of mass. The SUVs that contain only L-α-lecithin should have a net surface charge of zero, while those that contain 20% CL should have a negative surface charge. The tyrosine fluorescence of ALDH(−RGP) and thiolase[1−21] was enhanced upon interaction with SUVs, while the tryptophan fluorescence of rhodanese[1−23] was quenched. For each of the peptides, the fluorescence change in the presence of L-α-lecithin SUVs was smaller than what was observed with 20% CL (Figure 2). This relationship was most notable for thiolase[1−21] and ALDH(−RGP), clearly indicating that these peptides interacted more readily with vesicles contain-

Table 1: Secondary Structure of Rhodanese[1−23], Thiolase[1−21] and ALDH(−RGP) in Structure-Promoting Media[a]

	medium									
	buffer (50 mM P_i)		SDS (20 mM)		DPC (20 mM)		SUVs (0% CL)		SUVs (20% CL)	
peptide	α	β	α	β	α	β	α	β	α	β
rhodanese[1−23]	10[b]	nd[c]	66	0	75	5	23[b]	nd	70	1
thiolase[1−21]	4[b]	nd	32	31	29	34	1	36	15	62
ALDH(−RGP)	12[b]	nd	23	5	25	18	4	45	34	0

[a] Values under each heading are α-helix and β-strand percentages, respectively, calculated as described in Yang *et al*. (1986). [b] Percent helicity calculated from the mean residue ellipticity, as described in the text. [c]Not determined.

ing a negative charge. All of the peptides interacted with SUVs containing 20% CL, but with different affinities. The concentrations of half-maximal fluorescence change span an approximately 10-fold range. Rhodanese[1−23] appeared to have the greatest affinity for the SUVs, followed by ALDH(−RGP) and thiolase[1−21]. However, the stoichiometry of the interaction between rhodanese[1−23] and 20% CL SUVs appeared to be 1 peptide molecule to only five lipid molecules. To investigate the cause of this unusually high peptide/lipid ratio, the peptide was titrated with an aqueous suspension of lipids (80% L-α-lecithin/20% CL). With the lipid suspension, a similar titration curve was observed. In addition, a solution of 20% CL SUVs was titrated with rhodanese[1−23], resulting in data that showed the same stoichiometry. These results seem to indicate that rhodanese[1−23], but not the other peptides, was able to interact with lipids that were not preformed into bilayers. The nature of the interaction of this peptide with lipids is somehow different from the interaction that occurs with the other peptides.

Fluorescence titrations with detergents were difficult to interpret because, at the beginning of the titration, when detergent concentrations were low, the detergent had a denaturant effect on peptide secondary structure. When the critical micelle concentration was reached, and the detergent formed micelles, there was already a large excess of micelles, so it was only possible to observe the titration end point and not the informative part of the experiment that preceded it. However, it was possible to see that, with both DPC and SDS, the tryptophan fluorescence of rhodanese[1−23] was quenched and the tyrosine fluorescence of ALDH(−RGP) and thiolase[1−21] was enhanced at the titration end points. The net fluorescence changes were consistent with the titrations involving SUVs.

Circular Dichroism. Circular dichroism spectra were obtained for all of the peptides in aqueous buffer, the presence of SDS micelles, DPC micelles, SUVs composed of only L-α-lecithin, and SUVs made from a 80/20 mixture of L-α-lecithin and CL. The calculated α-helical and β-strand contents of the peptides for each condition are presented in Table 1. The peptides formed only a small amount of regular secondary structure when dissolved in phosphate buffer. Only rhodanese[1−23] displayed secondary structure characteristics in the presence of the lecithin SUVs. The spectrum could only be observed at wavelengths greater than 200 nm, so the helical content had to be estimated from the ellipticity at 222 nm. Using standard values of $[\Theta]_{222}$ for entirely helical and coiled peptides (Park *et al.*, 1993), the helix/coil ratio was calculated, giving a helical content for rhodanese[1−23] of approximately 23% in this environment, a value much less than what was observed in the presence of CL. Each of the peptides formed regular secondary structure in the presence of the other membrane-mimetic lipids. Rhodanese[1−23] and ALDH(−RGP) were predominantly helical in all the structure-promoting environments. In contrast, thiolase[1−21] had α-helical and β-strand content that appeared to be nearly equivalent in micellar solutions and contained mainly β-structure when bound to SUVs.

The extent of helix in 20% CL SUVs cannot be compared among the three peptides, since under the experimental conditions required to measure CD spectra insufficient lipid was present for ALDH(−RGP) and thiolase[1−21] to be in a state of maximal binding (see Materials and Methods). Within this limitation, surface charge appeared to be important for helix formation with SUVs, while there was little dependence on head group charge in the micellar interaction.

NMR Spectroscopy. The chemical shifts of protons in ALDH(−RGP) (Thornton *et al*., 1993) and thiolase[1−21] (Hammen *et al*., 1994) in the presence of micelles have been reported previously. The NMR spectrum of rhodanese[1−23] was characterized only in a 50% (v/v) aqueous solution of trifluoroethanol (TFE) (Hammen *et al*., 1994). Spectra of rhodanese[1−23] with micelles have now been obtained. Proton chemical shifts appear in Table 2. Sequential and medium-range contacts were found in the NOESY spectrum and are shown in Figure 3. The deduced secondary structure was α-helical between residues Val2 and Ser22.

For all three peptides, the rate of amide proton exchange with solvent was observed in the presence of DPC-d_{38} micelles. Two different initial states were used for these measurements. The first state was the preformed peptide−micelle complex (method I). The second began with uncomplexed micelle and peptide, and monitored exchange in competition with the formation of the complex (method II).

To ensure that the final state of the system was in equilibrium and that the complex formed was independent of the method used for complex preparation, the chemical shifts of α-protons were measured for the spectra of each peptide in methods I and II. These shifts are used routinely to assess secondary structure in polypeptides (Wishart *et al*., 1992). Chemical shift differences observed between the two protocols would indicate that the α-protons experience different environments and therefore the peptide−micelle complexes are not the same. When methods I and II were compared, the α-proton chemical shifts were essentially identical. The largest single difference was 0.02 ppm, and the majority were 0.00 ppm. The negligible differences between spectra obtained using methods I and II are evidence that the peptides are in the same final equilibrium conformation when observed by the two methods.

Table 2: Chemical Shift Assignments for Rhodanese[1−23] in the Presence of DPC Micelles

residue	NH	Hα	Hβ	Hγ	others
Met1	NO[a]	4.15	2.19,2.19	2.53,2.53	
Val2	8.98	3.95	2.12	1.01,0.89	
His3	8.34	4.52	3.26,3.21		7.28;7.15
Gln4	8.41	4.14	2.14,2.14	2.51,2.36	7.65, _[b]
Val5	8.14	3.74	2.24	1.06,0.94	
Leu6	8.01	4.03	1.78,1.62	1.76 or 1.16	0.88,0.74
Tyr7	8.24	4.12	3.10,3.10		7.04;6.78
Arg8	8.02	3.93	1.99,1.99	1.85,1.72	7.56;3.21,3.21
Ala9	8.33	3.91	1.44		
Leu10	8.13	4.03	1.80,1.63	1.76	0.89;0.85
Val11	8.10	3.62	2.05	0.83,0.76	
Ser12	8.05	4.41	4.02,3.92		
Thr13	7.96	3.96	4.20	1.15	
Lys14	8.17	3.93	1.99,1.86	1.46,1.37	2.88,2.88;1.68,1.68
Trp15	7.95	4.30	3.51,3.41		NO;7.58;7.49;7.35; 7.12;6.98
Leu16	8.16	3.66	1.73,1.68	1.61	0.87;0.87
Ala17	8.34	4.06	1.49		
Glu18	8.22	4.04	2.08,2.08	2.61,2.49	
Ser19	7.95	4.11	3.63,3.54		
Ile20	7.83	3.84	1.88	1.64,1.12,0.87	0.79
Arg21	7.93	4.14	1.94,1.81	1.73,1.65	7.57;3.14,3.14
Ser22	8.05	4.36	3.91,3.91		
Gly23	8.18	4.04, 3.93			_[b], _[b]

[a] Not observed. [b] Not assigned.

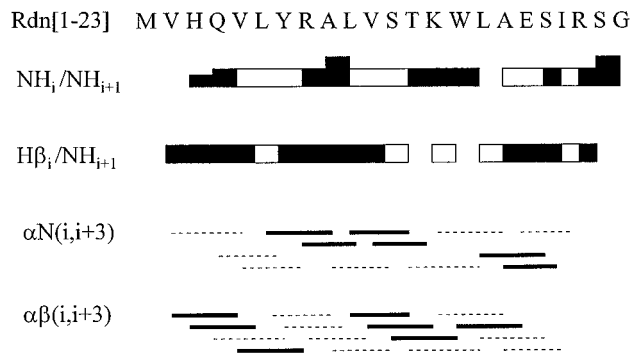

FIGURE 3: Sequential NOE contacts observed for rhodanese[1−23] in the presence of DPC micelles. The heights of bars in the NH_i/NH_{i+1} and β_i/NH_{i+1} rows indicate relative cross-peak intensity. Shaded areas indicate resolved cross-peaks with a unique assignment, while unshaded areas indicate that the cross-peak was present but the assignment was not unique. For the $i,i+3$ interactions, the solid line indicates the unique assignment while the dashed line indicates that a unique assignment could not be made.

The rate constants for exchange with solvent are shown for each peptide in Table 3 along with the correlation coefficient for the linear fit of the data. Some of the most slowly exchanging NHs, such as Val11 of rhodanese[1−23] did not have high correlation coefficients because few data points were obtained at large time values, when the intensities were changing. Regardless of the poor linear fit of the data, these resonances exchange very slowly, since the cross-peak intensities had changed to only a small degree after 20 h. From the rate constants (k_{ex}) and the amino acid sequences, exchange protection factors (PF) were calculated (Bai *et al.*, 1993). The intrinsic rate constants (k_{intr}) used

$$PF = k_{intr}/k_{ex}$$

were for buffered aqueous solution (0.1 M ionic strength) at 25 °C, which are similar to the conditions used in the present study. Protection factors obtained for each of the peptides

Table 3: Exchange Rate Constants ($\times 10^3$ min^{-1}) Observed for Amide Protons in Rhodanese[1−23], ALDH(−RGP), and Thiolase[1−21]

residue	k_{ex} (TFE)	r^2	k_{ex} (method II)	r^2	k_{ex} (method I)	r^2
rhodanese[1−23]						
Val5	>100[a]	nc[b]	>60	nc	7	nc
Leu6	17	nc	>60	nc	6	nc
Tyr7	4.75	0.979	>60	nc	2.24	0.966
Arg8	6.02	0.872	4.67	0.995	1.71	0.882
Ala9	7.05	0.978	35	nc	2.32	0.994
Leu10	2.7	0.995	3.71	0.992	1.88	0.960
Val11	0.35	0.667	0.58	0.981	1.31	0.940
Ser12	2.2	0.994	3.39	0.842	1.65	0.963
Thr13	7.5	0.988	>60	nc	>30	nc
Lys14	8.89	0.997	>60	nc	1.68	0.997
Trp15	2.07	0.992	28	nc	6	nc
Leu16	1.27	0.954	1.03	0.984	1.71	0.987
Ala17	1.46	0.948	>60	nc	2.72	0.979
Glu18	2.7	0.970	0.55	0.987	0.37	0.964
Ser19	4.94	0.975	7	nc	7	nc
Ile20	2.39	0.941	3.8	0.935	3.5	nc
Arg21	9	nc	6	nc	7	nc
Ser22	>100	nc	3.1	0.998	7	nc
ALDH(−RGP)[c]						
Leu12			20	nc	20	nc
Leu15			1.8	0.890	1.8	0.995
Leu16			2.1	0.920	1.1	0.973
Tyr18			30	nc	30	nc
Ala19			30	nc	30	nc
thiolase[1−21]						
Val7			30	nc	30	nc
Phe8			30	nc	30	nc
Ile9			30	nc	30	nc
Val10			2	nc	2	nc
Ala11			30	nc	30	nc
Ala12			30	nc	30	nc

[a] Not calculated because there were fewer than three data points. The rate constant was obtained from an estimation of the half-time for peak disappearance determined from inspection of the spectra. [b] A peak was not observed, so the value has a lower bound due to the time between mixing and the acquisition of the first spectrum. [c] Data for ALDH(−RGP) and thiolase[1−21] were not obtained in TFE.

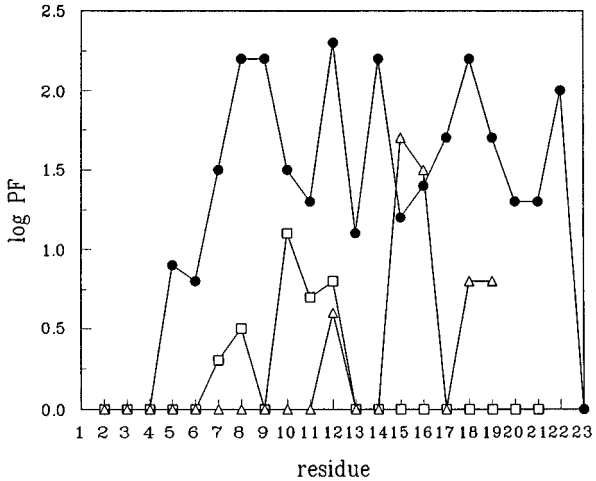

FIGURE 4: Logarithm of exchange protection factors plotted against amino acid position for rhodanese[1−23] (●), ALDH(−RGP) (△), and thiolase[1−21] (□) from rate constants measured using method I.

with method I are plotted versus sequence position in Figure 4; protection factors obtained using method II are plotted in Figure 5. Of the three peptides, rhodanese[1−23] made the strongest contact with the micelles, judging the extensive amount of exchange protection. The differences among the largest protection factors for each peptide, in Figure 4, show that the interaction affinities span about 1 order of magnitude.

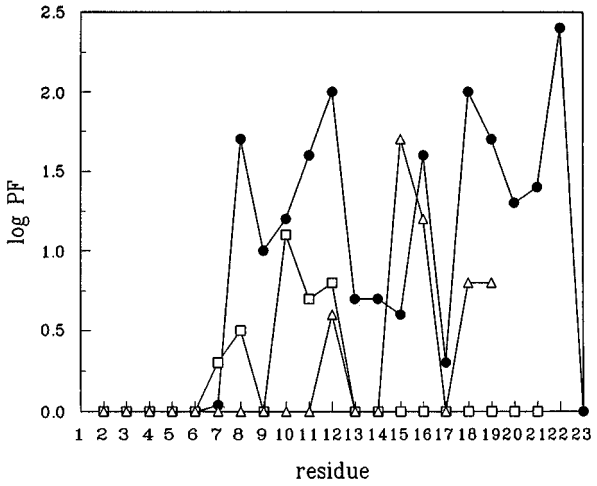

FIGURE 5: Logarithm of exchange protection factors plotted against amino acid position for rhodanese[1−23] (●), ALDH(−RGP) (△), and thiolase[1−21] (□) from rate constants measured using method II.

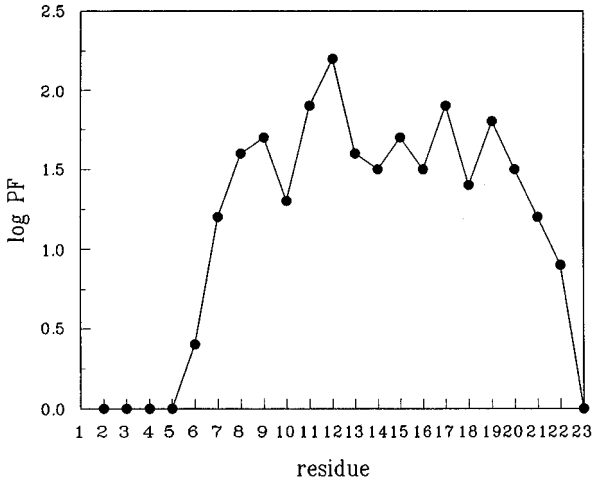

FIGURE 6: Logarithm of exchange protection factors plotted against amino acid position for rhodanese[1−23] in a 50% (v/v) mixture of 50 mM potassium phosphate buffer (pH 3.3) and trifluoroethanol.

Somewhat different patterns of protection resulted for rhodanese[1−23] when exchange was measured by the two different methods. In the data obtained from method I, the broad pattern of protection of the residues from Val5 to Ser22 is consistent with the burial of this section of the peptide within the micelle, rather than its lying along the micelle surface. With this type of interaction, consecutive amide protons can be excluded from contact with solvent. Among the protons with the fastest exchange rates were Val5, Leu6, Thr13, Ser19, Arg21, and Ser22. Intrinsic rates predicted for Ser19, Arg21, and Ser22 are fast because functional groups in adjacent side chains are able to catalyze the exchange reaction (Molday *et al*., 1972). Therefore, even though these amide protons were observed only in the first spectra of each experiment, their protection factors were high. In contrast, the poorest exchange protection was found for Val5, Leu6, and Thr13. Small protection factors for Val5 and Leu6 can be explained as effects on exchange near the ends of the helix where the contact with solvent is likely to be greatest. When the exchange experiment was carried out in a 1/1 (v/v) mixture of trifluoroethanol and water, a medium in which the peptide is known to be helical (Hammen *et al*., 1994), a similar protection pattern was observed (Figure 6). In solvent, the observed exchange protection can be attributed to stable hydrogen bond formation in the helical structure. In aqueous buffer alone, no cross-peaks were observed in the first spectrum of the experiment, showing that there was no observable intrinsic helical structure in this peptide. In the presence of micelles, resistance to exchange is due to the combination of hydrogen bonding and reduced solvent exposure. There was greater variation in the protection factors from method II (Figure 5). The broad pattern of protection seen for the preformed complex and in the aqueous TFE solution was not evident. The residues most protected from exchange in this experiment were Arg8, Val11, Ser12, Leu16, Glu18, Ser19, and Ser22. The distribution of these residues about the helical axis is restricted to approximately one-half of the circumference of the helical wheel shown in Figure 1.

Both ALDH(−RGP) and thiolase[1−21] showed similar protection patterns regardless of whether the data were gathered by method I or II. The C-terminal portion, residues 12−16, of ALDH(−RGP) contained the only amide protons that were protected from exchange. The significant protection of Leu15 and Leu16 shows that these residues made the strongest contact with the micelle (method I) and were also the first to interact with the micelle (method II). The lack of protection for Ser13 and Arg14 suggests that the peptide was located near the surface of the micelle and that the amide protons on the solvent-exposed, hydrophilic face of the helical peptide were available for exchange. For thiolase[1−21], the region of the peptide around Val10 appeared to make the only observable contact with the micelle. Relatively little protection from exchange was observed by either method I or II.

DISCUSSION

The three peptides employed in this study all function as presequences which allow a protein to enter mitochondria. Previous work showed that each was essentially structureless in aqueous solution but would form a helix in trifluoroethanol/water mixtures or in the presence of detergent micelles (Thornton *et al*., 1993; Hammen *et al*., 1994). Though it is not known if the presequence actually forms an ordered structure when it binds to the mitochondrial membrane or protein translocator, other sequences which we found not to function in import did not form ordered structures in the same helix-stabilizing milieu (Wang & Weiner, 1994). Thus, the ability of the presequence peptides to form an ordered structure and bind to lipid bilayers appears to correlate with their ability to perform import as part of a precursor protein.

From a thermodynamic perspective, the interaction between a positively charged polypeptide and a membrane can be separated into ionic and hydrophobic components. The ionic contribution to the peptide−membrane interaction has been shown to depend on the electrostatic surface potential, Ψ (Swanson & Roise, 1992; Thorgeirsson *et al*., 1995). The magnitude of the hydrophobic contribution should be proportional to the hydrophobic surface area that can be buried in the lipid bilayer, although the amount of stabilization achieved per unit of surface area is under debate (Reynolds *et al*., 1974; Sharp *et al*., 1991; White & Wimley, 1994). It has been proposed that the initial interaction between a positively charged polypeptide and the membrane surface is governed by a diffusion-controlled electrostatic attraction

(Wang & Weiner, 1994). The subsequent insertion of the hydrophobic portion of the peptide into the bilayer is energetically favorable (Engelman & Steitz, 1981). The stage in this process at which secondary structure is adopted is not clearly understood. Since the free energy difference of the helix−coil transformation in aqueous solution is near zero, the formation of secondary structure prior to insertion is reasonable (Jähnig, 1983; Engelman & Steitz, 1981). It has been suggested, however, that the formation of an ordered structure is promoted by the interaction of the peptide with the membrane surface (Jacobs & White, 1989). According to this model of interaction, when insertion of the amphiphilic peptide is complete, nonpolar side chains are located preferentially within the lipid bilayer, essentially removing them from contact with the solvent (Roise, 1993; Thornton *et al*., 1993). Amino acid residues with hydrophilic side chains maintain positions near the membrane surface, which allows them to form necessary stabilizing hydrogen bonds.

The surface charge of micelles and SUVs appears to have a different influence on the binding of the peptides used in this study. The fluorescence and CD data showed an enhancement of the interaction when the SUVs had a negative surface charge provided by CL. Both binding and helical structure formation are significantly lowered in the absence of CL, as we have shown with other presequence peptides (Wang & Weiner, 1993; Hammen *et al*., 1994). In contrast to the case involving peptides and SUVs, the CD spectra of peptide−micelle mixtures show no clear dependence on head group charge, since regular secondary structures are formed in the presence of both negative and formally neutral detergents. This difference suggests that electrostatic attraction is not as critical for peptide−micelle complex formation as it is for the peptide−bilayer interaction. The lack of influence by surface charge on peptide−micelle complex formation could be due to the lower packing density of phospholipids in micelles as compared to that in SUVs (Dill & Flory, 1981) or the reorganization of uniform micelles into mixed micellar aggregates that include the peptide. The micellar surface may be more readily penetrated by nonpolar peptide side chains as the complex forms. In this way, the thermodynamic benefits of removal of the hydrophobic groups from contact with solvent may be realized without passage of the peptide through a layer of charged functional groups at the vesicle surface.

Although micelles and SUVs show a different head group charge dependence in their interaction with rhodanese[1−23], ALDH(−RGP), and thiolase[1−21], they exhibit the same relative affinity for the three peptides. Fluorescence titrations with SUVs containing 20% CL show that rhodanese-[1−23] has the greatest affinity for the vesicles and that ALDH(−RGP) and thiolase[1−21] have lesser affinities, respectively. Amide proton exchange experiments utilizing method I exhibit the same relative affinity in the peptide−micelle interaction. The protection factors for rhodanese-[1−23] are greatest, followed by those for ALDH(−RGP) and then thiolase[1−21]. The trend follows the number of helical turns adopted by the three peptides (five, four, and three).

The hydrophobic contribution to the interaction between the peptides and micelles or SUVs should depend on the amount of hydrophobic surface area that is inserted into a lipid environment (Jorgensen *et al*., 1985). To assess the potential for hydrophobic surface burial, the solvent-exposed

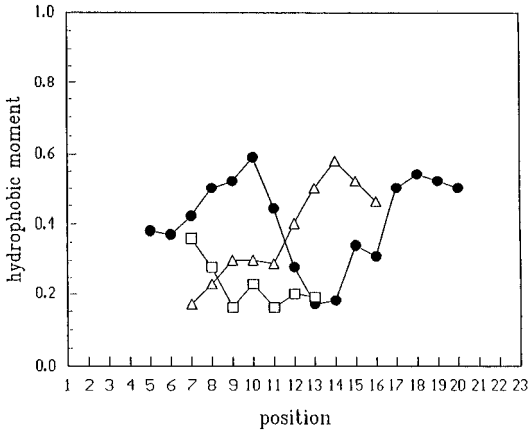

FIGURE 7: Plots of helical hydrophobic moment versus amino acid sequence for rhodanese[1-23] (●), ALDH(−RGP) (△), and thiolase-[1−21] (□). The hydrophobic moments were calculated for eight residue segments. The moment for each segment is plotted above the central fifth residue of that segment.

surface area was computed for the helical portion of each peptide in its experimentally determined conformation using computer-assisted molecular modeling. It was calculated that thiolase[1−21] had the largest exposed hydrophobic surface area, at 1854 Å^2. Rhodanese[1−23] and ALDH(−RGP) had 1781 and 1421 Å^2 of exposed hydrophobic surface area, respectively. If hydrophobic surface area were the most important factor in determination of binding affinity, thiolase-[1−21] would have had the greatest affinity for micelles and SUVs.

Hydrophobic surface alone is not sufficient for the peptide to bind effectively. The helical wheel diagrams in Figure 1 indicate that the helical structures of rhodanese[1−23] and ALDH(−RGP) should be more amphiphilic than that of thiolase[1−21]. Therefore, it appears that amphiphilicity may correlate with binding affinity. A more quantitative assessment of amphiphilicity is the hydrophobic moment (Eisenberg *et al*., 1982). Helical hydrophobic moments of the peptides, calculated in eight residue segments, are plotted versus sequence position in Figure 7. The helical regions of rhodanese[1−23] and ALDH(−RGP) that have maximal hydrophobic moment are also the segments that show the greatest protection from exchange upon interaction with micelles. No segment of thiolase[1−21] that is part of the helical structure has a comparable hydrophobic moment, and this peptide shows the lowest affinity for both micelles and SUVs. On the basis of the exchange data, it is the most hydrophobic segment of thiolase[1−21], as calculated by the Kyte−Doolittle hydropathy scale (Kyte & Doolittle, 1982), that interacts with the micelles.

It appears that the affinity of the interaction between peptides and micelles may be determined by the amphiphilicity of the peptide. In this case, affinity would not be simply a matter of hydrophobic surface or charge distribution, but the ability of the peptide to adopt an ordered structure which segregates hydrophilic from hydrophobic surfaces. Following this reasoning, the low affinity of thiolase[1−21] for both micelles and SUVs is due to the fact that the peptide can adopt many conformations that allow the insertion of hydrophobic side chains but none that include a regular secondary structure and proper orientation of the hydrophilic side chains.

On the basis of the exchange data, each peptide in this study uses the C-terminal portion of its helix for interaction

with micelles. The N-terminus of the peptide does not appear to be involved in the initial complex formation or in the complex that is eventually formed. The protection patterns obtained from the two different methods span a similar number of residues. In the complex measured by method I, the central part of rhodanese[1−23] appeared to be buried within the micelle with the exception of Thr13. One explanation for this observation is that the peptide must bend to allow it to remain buried in the micelle, and it bends near Thr13, disrupting the continuous stretch of helical hydrogen bonds. If the bend occurs near the solvent-exposed surface of the complex, the amide proton of Thr13 would be better able to exchange. The quenching of Trp15 fluorescence in rhodanese[1−23] upon interaction with 20% CL SUVs suggests that this residue is not buried in the lipid bilayer but is located near the surface of the vesicle. In the data from method II, Arg8, Val11, Ser12, Leu16, Glu18, Ser19, and Ser22 are the most protected amide protons. On the helical wheel diagram in Figure 1, these residues are all on one face of the helix. As shown in Figure 7, these positions also correspond to the peptide regions that have the largest helical hydrophobic moment. The peptide must be in a helical conformation when it enters the micelle initially for these residues to be protected, due to their spacing in the sequence. The initial penetration of this relatively hydrophilic face of the helix into the micelle is in accord with our other results which indicate that amphiphilic peptide characteristics are an important part of peptide−micelle complex formation. Unlike rhodanese[1−23], ALDH(−RGP) and thiolase[1−21] form the same type of complex with micelles whether exchange is observed by method I or II. ALDH(−RGP) appears to interact at the micellar surface due to the helical periodicity in the pattern of exchange protection observed in this study, and previously (Thornton *et al*., 1993). In this case, it is the more hydrophobic residues that are protected from exchange upon interaction with micelles. It is difficult to draw a specific conclusion on the position of thiolase[1−21] in the micelle on the basis of the limited exchange protection.

During the course of this study, it became apparent that a 1/1 correspondence between exchange rate constants and protection factors does not always exist. This conclusion could be readily seen in the results for Val11 and Leu16 in rhodanese[1−23], which were typically among the slowest exchanging amide protons, yet had relatively small protection factors. The magnitude of the protection factor depends on the intrinsic exchange rate constant calculated for a specific amino acid sequence in a random coil conformation. It has been shown that large side chains can effect exchange rates through a steric effect (Bai *et al*., 1993). This finding results in the calculation of a small intrinsic rate constant for both Val11 and Leu16, since they are both preceded in the sequence by bulky residues (Leu10 and Trp15). The accuracy of the protection factors is dependent on the assumption that the side chains have the same steric effect in the natural secondary structure, in this case a helix, as in the random coil conformation.

The study that we have described was undertaken initially to determine whether experimental data of peptides in a micellar milieu could be compared to studies of peptide−bilayer interactions. For technical reasons, it was not possible to do all experiments with each lipid environment, but we have found qualitatively similar results for the binding affinity of the three peptides to micelles and SUVs. The surface charge of the SUVs appeared to be more critical for the interaction with the peptides than head group charge of the detergents which formed micelles. Furthermore, this study has presented data that are consistent with the emerging view that amphiphilicity is a determining factor in peptide−membrane interactions (Roise, 1993). The data also indicated that rhodanese[1−23] adopted a helical conformation before entering the complex with the micelle. It was interesting to note that rhodanese[1−23] appeared to make initial contact with micelles using a relatively hydrophilic surface, while ALDH(−RGP) and thiolase[1−21] appear to make initial contact with hydrophobic residues. This difference may reflect a variation in the type of interaction among the three peptides which was also observed in their binding to SUVs. Our earlier hypothesis, based on one presequence, was that the C-terminal portion of the presequence was involved with membrane interaction (Karslake *et al*., 1991). On the basis of the data we now have, it appears that the interaction with membrane surfaces may depend on the location of an amphiphilic region of the sequence that is near but not necessarily at the C-terminus.

REFERENCES

Bai, Y., Milne, J. S., Mayne, L., & Englander, S. W. (1993) *Proteins 17*, 75−86.

Bax, A., & Davis, D. G. (1985) *J. Magn. Reson. 65*, 355−360.

Braun, W., Bosch, C., Brown, L. R., Go, N., & Wüthrich, K. (1981) *Biochim. Biophys. Acta 667*, 377−396.

Braun, W., Wider, G., Lee, K. H., & Wüthrich, K. (1983) *J. Mol. Biol. 169*, 921−948.

Cramer, W. A., Engelman, D. M., von Heijne, G., & Rees, D. C. (1992) *FASEB J. 6*, 3397−3402.

De Kroon, A. I. P. M., de Gier, J., & de Kruijff, B. (1993) in *Protein-Lipid Interactions* (Watts, A., Ed.) pp 107−127, Elsevier Science, Amsterdam.

Dill, K., & Flory, P. (1981) *Proc. Natl. Acad. Sci. U.S.A. 78*, 676−680.

Eisenberg, D., Weiss, R. M., Terwilliger, T. C., & Wilcox, W. (1982*) Faraday Symp. Chem. Soc. 17*, 109−120.

Engelman, D. M., & Steitz, T. A. (1981) *Cell 23*, 411−422.

Englander, S. W., & Mayne, L. (1992) *Annu. Rev. Biophys. Biomol. Struct. 21*, 243−265.

Gierasch, L. M., Lacy, J. E., Thompson, K. F., Rockwell, A. L., & Watnick, P. I. (1982) *Biophys. J. 37*, 275−284.

Glaser, S. M. & Cumsky, M. G. (1990) *J. Biol. Chem. 265*, 8808−8816.

Hammen, P. K., Gorenstein, D. G., & Weiner, H. (1994) *Biochemistry 33*, 8610−8617.

Haucke, V., Lithgow, T., Rospert, S., Hahne, K., & Schatz, G. (1995) *J. Biol. Chem. 270*, 5565−5570.

Jacobs, R. E., & White, S. H. (1989) *Biochemistry 28*, 3421−3437.

Jähnig, F. (1983) *Proc. Natl. Acad. Sci. U.S.A. 80*, 3691−3695.

Jeener, J., Meier, B. H., Bachmann, P., & Ernst, R. R. (1979) *J. Chem. Phys. 71*, 4546−4553.

Jorgensen, W. L., Gao, J., & Ravimohan, C. (1985) *J. Phys. Chem. 89*, 3470−3473.

Karslake, C., Piotto, M., Pak, Y. K., Weiner, H., & Gorenstein, D. G. (1990) *Biochemistry 29*, 9872−9878.

Kim, J., Mosior, M., Chung, L. A., Wu, H., & McLaughlin, S. (1991) *Biophys. J. 60*, 135−148.

Kyte, J., & Doolittle, R. F. (1982) *J. Mol. Biol. 157*, 105−132.

Landry, S. J., & Gierasch, L. M. (1991) *Biochemistry 30*, 7359−7362.

Molday, R. S., Englander, S. W., & Kallen, R. G. (1972) *Biochemistry 11*, 150−158.

Myers, M., Mayorga, O. L., Emtage, J., & Freire, E. (1987) *Biochemistry 26*, 4309−4315.

Opella, S. J., Kim, Y., & McDonnell, P. (1994) *Methods Enzymol. 239*, 536−560.

Ou, W., Ito, A., Okazaki, H., Omura, T. (1989) *EMBO J. 8*, 2605−2612.
Pak, Y. K., & Weiner, H. (1990) *J. Biol. Chem. 265*, 14298−14307.
Park, S.-H., Shalongo, W., & Stellwagen, E. (1993) *Biochemistry 32*, 7048−7053.
Piatini, U., Sørensen, O., & Ernst, R. R. (1983) *J. Am. Chem. Soc. 105*, 6800−6801.
Reynolds, J. A., Gilbert, D. B., & Tanford, C. (1974) *Proc. Natl. Acad. Sci. U.S.A. 71*, 2925−2927.
Roise, D. (1993) in *Thermodynamics of Membrane Receptors and Channels* (Jackson, M. B., Ed.) pp 81−125, CRC Press, Boca Raton, FL.
Roise, D., Theiler, F., Horvath, S. J., Tomich, J. M., Richards, J. H., Allison, D. S., & Schatz, G. (1988) *EMBO J. 7*, 649−653.
Saier, M. H., Jr., Werner, P. K., & Muller, M. (1989) *Microbiol. Rev. 53*, 333−366.
Sargent, D. F., & Schwyzer, R. (1991) *Proc. Natl. Acad. Sci. U.S.A. 83*, 5774−5778.
Schwyzer, R. (1991) *Biopolymers 31*, 785−792.
Sharp, K. A., Nicholls, A., Fine, R. F., & Honig, B. (1991) *Science 252*, 106−109.
Smallcombe, S. H. (1993) *J. Am. Chem. Soc. 115*, 4776−4785.
Snel, M. M. E., de Kroon, A. I. P. M., & Marsh, D. (1995) *Biochemistry 34*, 3605−3613.
Swanson, S. T., & Roise, D. (1992) *Biochemistry 31*, 5746−5751.
Thorgeirsson, T. E., Yu, Y. G., & Shin, Y.-K. (1995) *Biochemistry 34*, 5518−5522.
Thornton, K., & Gorenstein, D. G. (1994) *Biochemistry 33*, 3532−3539.
Thornton, K., Wang, Y., Weiner, H., & Gorenstein, D. (1993) *J. Biol. Chem. 268*, 19906−19914.
Vallette, F. M., Juin, P., Pelleschi, M., & Henry, J.-P. (1994) *J. Biol. Chem. 269*, 13367−13374.
Von Heijne, G. (1986) *EMBO J. 5*, 1335−1342.
Wang, Y., & Weiner, H. (1994) *Biochemistry 33*, 12860−12867.
Wang, Y., & Weiner, H. (1993) *J. Biol. Chem. 268*, 4759−4765.
Wang, Y. (1994) Ph.D. Dissertation, Purdue University, West Lafayette, IN.
White, S. H., & Wimley, W. C. (1994) *Curr. Opin Struct. Biol. 4*, 79−86.
Wickner, W. (1988) *Biochemistry 27*, 1081−1086.
Wishart, D. S., Sykes, B. D., & Richards, F. M. (1991) *J. Mol. Biol. 222*, 311−333.
Yang, J. T., Wu, C.-S. C., & Martinez, H. M. (1986) *Methods Enzymol. 130*, 208−269.

BI951848G